Journal of
Medicinal Chemistry

Article

(6,7-Dimethoxy-2,4-dihydroindeno[1,2-*c*]pyrazol-3-yl)phenylamines: Platelet-Derived Growth Factor Receptor Tyrosine Kinase Inhibitors with Broad Antiproliferative Activity against Tumor Cells

Chih Y. Ho, Donald W. Ludovici, Umar S. M. Maharoof, Jay Mei, Jan L. Sechler, Robert W. Tuman, Eric D. Strobel, Laura Andraka, Hwa-Kwo Yen, Gregory Leo, Jian Li, Harold Almond, Hong Lu, Ann DeVine, Rose M. Tominovich, Judith Baker, Stuart Emanuel, Robert H. Gruninger, Steven A. Middleton, Dana L. Johnson, and Robert A. Galemmo

J. Med. Chem., **2005**, 48 (26), 8163-8173• DOI: 10.1021/jm050680m • Publication Date (Web): 22 November 2005

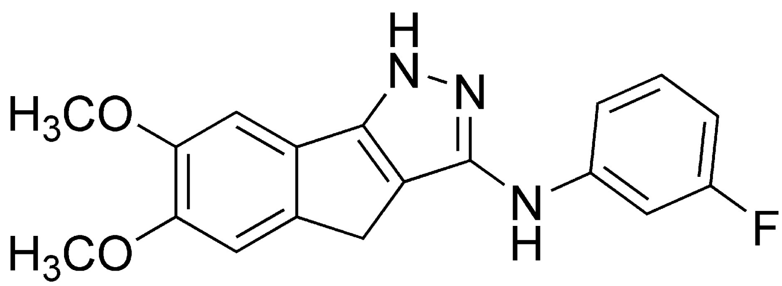

17: JNJ-10198409

(6,7-Dimethoxy-2,4-dihydroindeno[1,2-*c*]pyrazol-3-yl)phenylamines: Platelet-Derived Growth Factor Receptor Tyrosine Kinase Inhibitors with Broad Antiproliferative Activity against Tumor Cells

Chih Y. Ho,[‡] Donald W. Ludovici,[‡] Umar S. M. Maharoof,[‡] Jay Mei,[‡] Jan L. Sechler,[‡] Robert W. Tuman,[‡] Eric D. Strobel,[‡] Laura Andraka,[‡] Hwa-Kwo Yen,[§] Gregory Leo,[‖] Jian Li,[†] Harold Almond,[†] Hong Lu,[‡] Ann DeVine,[‡] Rose M. Tominovich,[‡] Judith Baker,[‡] Stuart Emanuel,[⊥] Robert H. Gruninger,[⊥] Steven A. Middleton,[⊥] Dana L. Johnson,[‡] and Robert A. Galemmo, Jr.[*,‡]

Oncology Research Team, High Throughput Chemistry Team, Molecular Design and Informatics Team, Analytical Research Team, Johnson & Johnson Pharmaceutical Research and Development, L.L.C., Spring House Research and Early Development Site, Welsh and McKean Roads, Spring House, Pennsylvania 19477, and Cancer Therapeutics Team, Johnson & Johnson Pharmaceutical Research and Development, L.L.C., Raritan Research and Early Development Site, Route 202, Raritan, New Jersey 08869

Received July 18, 2005

A series of (6,7-dimethoxy-2,4-dihydroindeno[1,2-*c*]pyrazol-3-yl)phenylamines has been optimized to preserve both potent kinase inhibition activity against the angiogenesis target, the receptor tyrosine kinase of *P*latelet-*D*erived *G*rowth *F*actor-BB (PDGF-BB), and to improve the broad tumor cell antiproliferative activity of these compounds. This series culminates in the discovery of **17** (JNJ-10198409), a compound with anti-PDGFR-β kinase activity (IC_{50} = 0.0042 μM) and potent antiproliferative activity in six of eight human tumor cell lines (IC_{50} < 0.033 μM).

Introduction

Angiogenesis, the formation of new blood vessels from preexisting vasculature, is fundamentally important for the physiology of neonatal development, reproduction, and wound healing; however, the pathophysiological contribution of this process to cancer has received much attention.[1] Folkman's seminal observation,[2] that the sustained growth of solid tumors beyond a few millimeters in diameter is dependent on the ability of tumor cells to recruit new blood vessels from the existing vascular network, has led to considerable efforts to develop agents capable of inhibiting tumor-induced angiogenesis as a therapeutic approach in oncology.[3] Among the many important endogenous stimulators of angiogenesis, PDGF-BB and its corresponding tyrosine kinase receptor PDGFR-β play an important role in the angiogenic process.[4−6] As a proangiogenic protein, PDGF-BB exerts both mitogenic and chemotactic effects on microvascular endothelial cells through the PDGF receptor tyrosine kinase-signaling pathway.[5,6] In addition, PDGF-BB can induce endothelial cells to express high levels of VEGF, another potent stimulator of angiogenesis.[7,8] PDGF-BB is an important mitogenic factor for smooth muscle cells and pericytes, important cell types that participate in the later stages of angiogenesis by surrounding endothelial cells to stabilize the newly formed microvessels.[8,9]

Circumstantial evidence also implicates PDGF as a driver of tumor cell proliferation in some cancers. Overexpression of PDGF and its receptors has been demonstrated in human cancers including lung,[10] breast,[11] colorectal,[12] glioma,[13] and esophageal.[14] PDGF and PDGF receptors are coexpressed on tumor vasculature and are up-regulated during tumor progression.[13] Elevated circulating levels of PDGF are associated with metastatic disease[15] and higher microvessel counts in human breast cancer.[16] Finally, PDGF receptor is expressed in both vascular endothelial cells and smooth muscle cells in the tumor stroma.[17]

The effects of PDGF-BB are mediated through ligand binding to its cell surface receptor tyrosine kinase, PDGFR-β, followed by receptor dimerization and autophosphorylation of the transmembrane tyrosine kinase domain.[18,19] This event activates several downstream signaling molecules and their pathways, including phospholipase-C-γ (PLC-γ), Grb2/Sos1, MAP kinase, GAP, Src, and PI3.[18−21] At the cellular level this activity evokes a diverse set of responses, including proliferation and chemotaxis in smooth muscle and endothelial cells as well as changes in endothelial cell morphology. A variety of experimental approaches have provided validation of the importance of the PDGF pathway and the potential as a therapeutic strategy for inhibiting tumor-induced angiogenesis and growth. These experimental approaches include the use of PDGF receptor antibodies,[22] peptidomimetics of PDGF[23,24] and small molecule inhibitors of PDGF receptor tyrosine kinase activity.[25−28]

One of the promising new concepts in antiangiogenic therapy is that antiangiogenic agents enhance the remodeling or 'normalization' of tumor vasculature.[29] It has been proposed that a regimen that includes an antiangiogenic agent with conventional chemotherapy will have enhanced efficacy because the 'normalized' tumor vascular bed more efficiently distributes chemotherapeutic agents to the tumor mass.[29] On the basis

* Corresponding author. Telephone: 610-458-6056. Fax: 610-458-8249. E-mail: rgalemmo@prdus.jnj.com.
‡ Oncology Research Team.
§ High Throughput Chemistry Team.
† Molecular Design and Informatics Team.
‖ Analytical Research Team.
⊥ Cancer Therapeutics Team.

10.1021/jm050680m CCC: $30.25
Published on Web 11/22/2005

Scheme 1. Preparation of Compounds **2**−**21**[a]

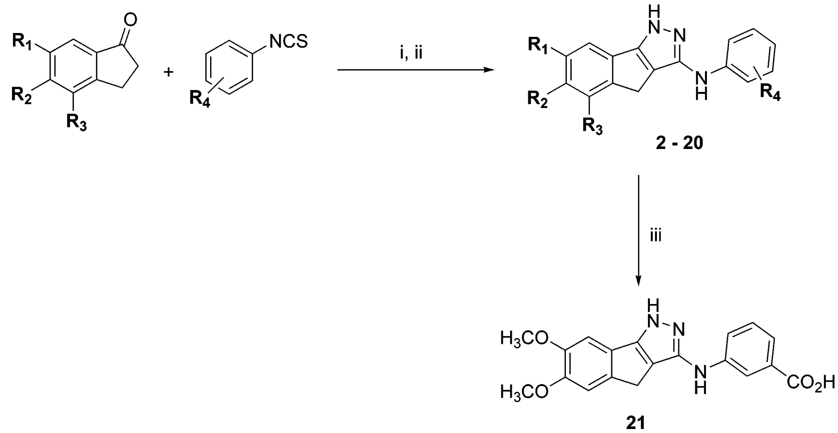

[a] (i) LHMDS, THF, RT, 12 h; (ii) NH_2NH_2, AcOH, reflux, 24 h, 40 to 70% for both steps; (iii) from **19** (R_4 = 3-CO_2CH_3): LiOH, THF, H_2O, 48 h, RT, 39%.

of this reasoning, we developed a strategy to discover agents that would have the potential to target both the tumor cell directly by an antiproliferative effect and serve as an antiangiogenic agent to promote the 'normalization' of the supporting tumor vasculature. In this paper we report a series of compounds that have the requisite antiproliferative activity and are putative antiangiogenic agents due to their inhibition of PDGFR-β tyrosine kinase.

Chemistry. The compounds used in these studies were prepared by a one-pot, two-step procedure starting from commercially available indan-1-ones and phenyl thioisocyanates (Scheme 1). A solution of the indanone and phenyl isothiocyanate in THF was added dropwise to lithium hexamethyldisilane in THF at room temperature. After 12 h, hydrazine and a small amount of acetic acid were added to the reaction and the mixture was heated at reflux for 24 h. Typical purified yields for the two-step procedure were in the range of 40% to 70%. The 3-carboxyphenyl analogue **21** was prepared in 39% yield from the corresponding methyl ester **19** by base hydrolysis.

Biology. Our testing cascade began with an assay of the PDGF receptor kinase activity by measuring the ability of the kinase to phosphorylate a biotinylated PLC1γ peptide containing the tyrosine substrate residue for PDGF RTK bound to a Streptavidin Flashplate in the presence of 5 μM ATP. The extent of phosphorylation was estimated from the amount of [^{33}P] retained after exposure to [^{33}P]-γ-ATP. The ability of *H*uman *C*oronary *A*rtery *S*mooth *M*uscle *C*ells (HCASMC) to incorporate [^{14}C]-thymidine upon proliferative stimulation by rh-PDGF-BB was used as a measure of the PDGF RTK inhibition activity of this series in intact cells. The inhibition of *L*ow *S*erum *G*rowth *S*upplement (LSGS)-induced proliferation of *H*uman *U*mbilical *V*ein *E*ndothelial *C*ells (HUVEC), cells not particularly responsive to stimulation by PDGF, was used as a measure of a compound's non-PDGF driven antiproliferative activity against nontransformed cells. A panel of human tumor cell lines, including AsPC-1 (pancreatic), PC3 (prostate), H460 (lung), LoVo (colon), A375 (melanoma), LnCAP (prostate), U87MG (glioma), and T47D (breast), was used to estimate the tumor cell growth inhibition activity of this series. Inhibition of tumor cell proliferation was determined by [^{14}C]-thymidine incorporation following 48 h exposure to compound.

Results and Discussion

Our interest was to develop antiangiogenic compounds with an additional antiproliferative activity capable of inhibiting tumor progression by controlling both the vascularization and proliferation of the tumor mass. Tumors may be regarded as a two-compartment system consisting of the vasculature supporting tumor growth composed of 'normal' homogeneous vascular endothelial cells, smooth muscle cells, and pericytes that are surrounded by colonies of neoplastic cancer cells. To find molecules that would affect both the vascular and transformed compartments, we identified several compounds with the potential to inhibit the PDGFR-β kinase-mediated angiogenic effect and then assayed them for collateral antiproliferative activity against a panel of human tumor cell lines.

Screening of the Johnson & Johnson compound library with an assay of PDGFR-β kinase inhibition led to the identification of **1** as a potent inhibitor of PDGFR-β kinase (Table 1, IC_{50} = 0.017 μM). Compound **1** also had modest tumor cell antiproliferative activity (IC_{50} < 10 μM) for six of eight tumor cell lines. Analogues of **1** have been reported previously,[30] nevertheless, because of the anti-PDGF and antiproliferative activity, **1** was useful as a starting point for the design of a novel compound series. We began by docking **1** in a homology model of the PDGF receptor kinase ATP binding site (Figures 1 and 2). This initial effort indicated that the PDGF kinase ATP binding site would readily accommodate the transmutation of compound **1** to a (2,4-dihydroindeno[1,2-*c*]pyrazole-3-yl)phenylamine such as **2**−**6** (Table 1). It was apparent that an additional H-bond donor interaction could be gained with the hinge region of the ATP binding site and the 3-aminophenyl substituent would be accommodated in a lipophillic region of the binding pocket. However, two issues hampered our efforts to develop a definitive binding model for this series. First, the pyrazole ring can form two N−H tautomers, making it difficult to assign the H-bonding network for this system. Second, docking the flat, rigid tricyclic 'body' of

Table 1. IC_{50} (μM) Values for PDGF Kinase Inhibition[a] and the Antiproliferative Activity against PDGF-BB-Stimulated HCASMC,[b] LSGS-Stimulated HUVEC,[c] and Human Tumor Cell Lines[d] for **1**–**6**

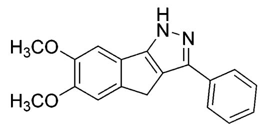

1

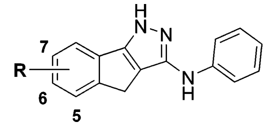

2-6

	R	PDGF RTK	HCASMC	HUVEC	H460	LoVo	LnCAP	PC3	T47D	A375	ASPC1	U87MG
1		0.017	0.124	1.39	8.4	2.7	1.2	31.2	4.41	8.85	6.82	> 50
2	6,7-di-OCH_3	0.009	0.023	0.031	0.353	0.124	0.60	0.108	0.42	0.062	2.16	21 (2)
3	H	0.317	–	–	–	–	–	–	–	–	–	–
4	7-OCH_3	0.018	0.009	0.015	9.95	10.53	14.37	> 10	> 10	> 50	> 10	> 100
5	6-OCH_3	0.217	–	–	–	–	–	–	–	–	–	–
6	5-OCH_3	0.054	0.487	0.283	2.8 (2)	0.798	1.7	7.34	4.7	1.19	> 10	> 100

[a] The IC_{50} values were determined using GraphPad Prism software and 95% confidence intervals for all data were in ranges of less than 2-fold of the reported values. The data were obtained in triplicate determinations at eight concentrations of compound in the presence of 5 μM ATP. [b] HCASMC proliferation was induced by stimulation with rh-PDGF BB and quantitated by measuring [^{14}C]-thymidine incorporation. The IC_{50} values were determined using GraphPad Prism software, and 95% confidence intervals for all data were in ranges of less than 2-fold of the reported values. The data were obtained in triplicate determinations at eight concentrations of compound. [c] HUVEC proliferation was induced by stimulation with LSGS and quantitated by measuring BrdU incorporation. The IC_{50} values were determined using GraphPad Prism software, and 95% confidence intervals for all data were in ranges of less than 2-fold of the reported values. The data were obtained using six serial dilutions of each compound with eight replications for each concentration. [d] The effects of compounds on tumor cells in log phase growth were measured by [^{14}C]-thymidine incorporation. The IC_{50} values were determined using GraphPad Prism software, and 95% confidence intervals for all data were in ranges of less than 2-fold of the reported values. The data were obtained in duplicate measurements at eight serial dilutions of each compound.

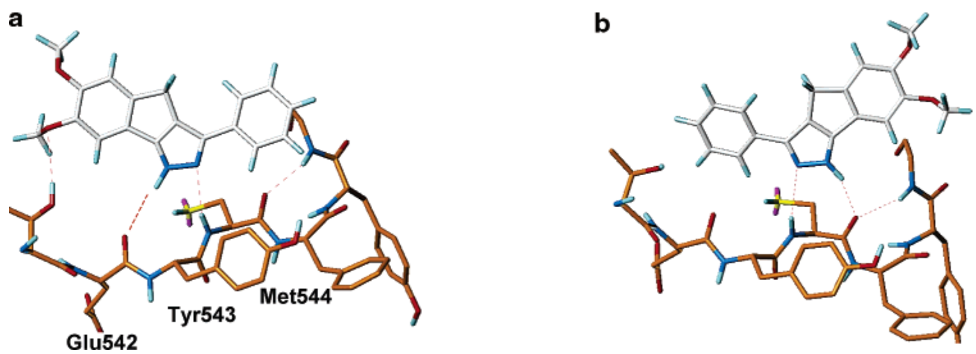

Figure 1. (a and b) Two possible binding orientations for **1**.

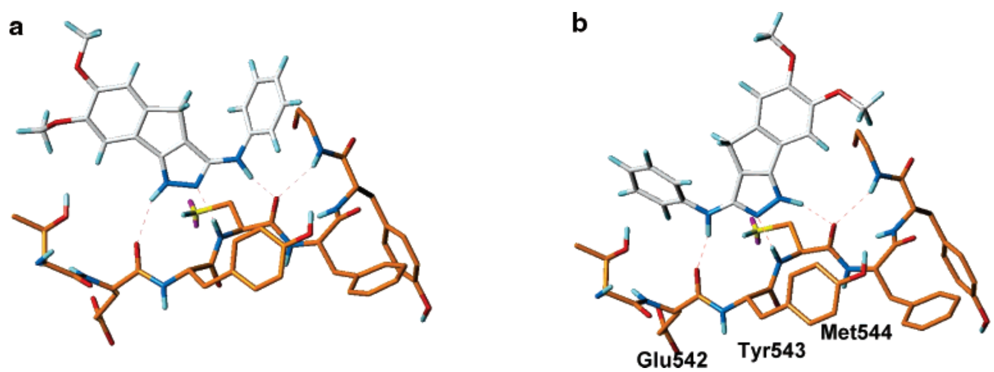

Figure 2. (a and b) Two possible binding orientations for **2**.

2 in the ATP binding site gives two energetically degenerate but opposite orientations. Our efforts to further clarify these issues and arrive at a definitive binding model are summarized at a later point in this report (vide infra).

As expected, the exchange of the 3-phenyl in **1** for the 3-aminophenyl group in **2** does preserve the PDGFR kinase inhibition activity. When **2** is shorn of the 6,7-dimethoxy groups, the resulting compound **3** is considerably less active as a kinase inhibitor (Table 1, PDGFR-β $IC_{50} = 0.317$ μM). To recover this activity, a systematic survey of the importance of methoxy substitution on kinase inhibition was undertaken. A series of three monomethoxy derivatives were prepared: 7-methoxy (**4**, PDGFR-β $IC_{50} = 0.018$ μM), 6-methoxy (**5**, PDGFR-β $IC_{50} = 0.217$ μM), and 5-methoxy (**6**, PDGFR-β $IC_{50} = 0.054$ μM). However, best results were obtained with the 6,7-dimethoxy substitution pattern of compound **2** (PDGFR-β $IC_{50} = 0.009$ μM).

Furthermore, compounds **2**, **4**, and **6** have activity in an assay of PDGF-BB stimulated HCASMC proliferation that parallels the activity in the isolated enzyme assay, suggesting that cell penetration is not an issue for this series. In a companion assay of LSGS-stimulated

Table 2. Effect of Substitution on 3′-Aminophenyl Group on the IC_{50} (μM) Values of PDGF Kinase Inhibition[a] and PDGF-BB-Stimulated HCASMC Proliferation[b]

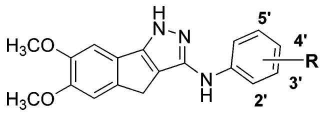

	R	PDGF RTK	HCASMC
7	2′-Cl	0.11	–
8	3′-Cl	0.003	0.268
9	4′-Cl	0.659	–
10	2′,5′-di-Cl	6.22 (2)	–
11	2′,4′-di-Cl	5.42 (2)	–
12	3′,4′-di-Cl	0.41 (2)	–
13	3′,5′-di-Cl	0.31 (2)	–
14	3′-OCH_3	0.010	0.016 (2)
15	3′-CH_3	0.012	0.188
16	3′-Br	0.005	0.032 (2)
17	3′-F	0.0042 + 0.00063 (11)	0.003 (2)
18	3′-CN	0.137	–
19	3′-CO_2CH_3	0.033	0.011 (2)
20	3′-CF_3	0.038	0.001
21	3′-CO_2H	> 0.8	

[a] The IC_{50} values were determined using GraphPad Prism software, and 95% confidence intervals for all data were in ranges of less than 2-fold of the reported values. The data were obtained in triplicate determinations at eight concentrations of compound in the presence of 5 μM ATP. [b] HCASMC proliferation was induced by stimulation with rh-PDGF BB and quantitated by measuring [^{14}C]-thymidine incorporation. The IC_{50} values were determined using GraphPad Prism software, and 95% confidence intervals for all data were in ranges of less than 2-fold of the reported values. The data were obtained in triplicate determinations at eight concentrations of compound.

HUVEC proliferation, a cell system *not* responsive to PDGF-BB, compounds **2**, **4**, and **6** have potent antiproliferative activity *not* dependent on PDGF-BB. We studied this non-PDGF-BB-mediated antiproliferative activity in the tumor cell panel (Table 1). The potent PDGF kinase inhibitors **4** and **6** are found to be poor inhibitors of tumor cell proliferation. However, the 6,7-dimethoxy compound, **2**, has good activity in these assays with $IC_{50} \leq 0.64$ μM in six tumor cell lines. This suggested that the tumor cell antiproliferative activity of **2** was not the result of its PDGFR-β kinase inhibition activity but must be due to another mechanism. To understand the SAR of both of these activities, a series of 6,7-dimethoxy analogues were prepared and examined for their PDGFR-β kinase inhibition and antiproliferative activity against tumor cells.

The effect of substitution of the 3-aminophenyl on PDGFR-β kinase inhibition activity was studied with a series of mono- and dichlorophenyl derivatives (Table 2, **7**−**13**). 2′-, 3′-, and 4′-Chlorophenyl analogues **7**-**9** demonstrate a clear preference for substitution in the 3′ position (**8**, PDGFR-β IC_{50}= 0.003 μM). Dichlorophenyl analogues with substitution at the 2′,5′- and 2′,4′-positions were compounds with inhibition activity in the micromolar range while 3′,4′- and 3′,5′- dichlorophenyl substitution gives inhibitors with kinase IC_{50} values of several hundred nanomolar.

Compounds **14**−**21** (Table 2) illustrate the effect of a variety of 3′-substituents on PDGFR-β kinase inhibition activity. Halogen substituents were preferred with the chloro (**8**), fluoro (**17**), and bromo (**16**), providing the most potent analogues (PDGFR-β IC_{50} < 0.010 μM). Intermediate potency was achieved with the methoxy (**14**), methyl (**15**), carboxymethyl (**19**), and trifluoromethyl (**20**) analogues (PDGFR-β IC_{50} > 0.010 μM < 0.10 μM). Poor potency was obtained with 3′-cyano substituent (**18**, PDGFR-β IC_{50} = 0.137 μM) and carboxylic acid (**21**, PDGFR-β IC_{50} > 0.8 μM).

The cellular potencies of these kinase inhibitors were studied in cell-proliferation assays using the 'normal' HCASMC cells (Table 2). In the HCASMC proliferation assay, driven by exogenous PDGF-BB, all compounds **8**, **14-20** inhibited ^{14}C-labeled thymidine incorporation over a broad range (IC_{50}s = 0.001 μM to 0.268 μM, Table 3), indicating good cell penetration for most of these compounds. However, the antiproliferative activity observed for many of these compounds in the LSGS-stimulated HUVEC assay and the panel of human tumor cells suggested a more complex cell activity profile for this series

With only a few exceptions, the potent kinase inhibitors (PDGFR-β IC_{50} < 0.05 μM) **8**, **14**−**17**, **19**, and **20** had antiproliferative IC_{50} < 0.05 μM (Table 3) for all tumor cells except the pancreatic cancer (ASPC1) and the glioblastoma (U87MG) cell lines. Comparison of the antiproliferative activity of **8**, **14**−**17**, **19**, and **20** in the panel of tumor cell lines with their activity against LSGS-stimulated HUVEC proliferation suggested that, for some of these compounds, the antiproliferative activity may be tumor cell selective. In the LSGS-stimulated HUVEC proliferation assay, the 3′-halo derivatives **8**, **16**, **17**, and the 3′-trifluoromethyl **20** were poor inhibitors of normal cell proliferation (IC_{50} > 1 μM); while **2**, the 3′-methoxy **14**, and the 3′-methyl **15** were potent inhibitors (IC_{50} < 0.10 μM).

The potent and selective antiproliferative activity against tumor cell lines indicated significant antitumor potential for these compounds. Therefore, the mechanism of the tumor cell selective antiproliferative activity observed for **8**, **16**, **17**, and **20** warranted closer examination. Compound **17** (JNJ-10198409) was chosen for further study based upon the potent PDGFR-β kinase inhibition (IC_{50}= 0.0042 μM), activity in PDGF-BB stimulated HCASMC assay (IC_{50}= 0.002 μM), poor activity against LSGS-stimulated HUVEC (IC_{50}= 4.87 μM), and excellent tumor cell antiproliferative activity (IC_{50} < 0.033 μM) in six of eight tumor cell lines.

Compound **17** is an ATP competitive inhibitor of PDGFR-β kinase as exhibited by the rightward shift of the dose response curve at increasing concentrations of ATP (data not shown).[31] In a battery of growth factor kinase inhibition assays **17** has good activity against PDGFR-α kinase (IC_{50} = 0.045 μM, Table 4), has poor activity against the VEGFR (IC_{50} = 3.1 μM) and bFGFR-1 kinases (IC_{50} = 45.8 μM), and is inactive against EGFR (IC_{50} > 100 μM) and HER-2 (IC_{50} > 10 μM) kinases. Like STI-571,[32] **17** is a potent inhibitor of the c-Abl kinase (IC_{50} = 0.022 μM). Workers at Bristol Meyers Squibb have reported a series of indenopyrazoles CDK4/CDK2 inhibitors with antiproliferative activity against human and murine tumor cell lines.[33] Unlike the Bristol Myers Squibb inhibitors, the kinase profile for **17** indicates that this compound lacks significant CDK inhibition activity (IC_{50} > 10 μM for CDKs-1, -2, -4, and -7), suggesting inhibition of this enzyme family cannot account for the observed antiproliferative activity in this series. Compound **17** does have modest activity against c-Src (IC_{50} = 0.185 μM), Lck (IC_{50} = 0.10 μM),

Table 3. IC_{50} (μM) Values of Inhibition of LSGS-Stimulated HUVEC Proliferation[a] and Human Tumor Cell Proliferation[b] for **2**, **8**, **14**−**17**, and **20**

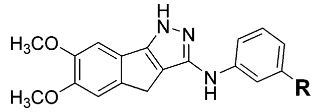

	R	HUVEC	H460	LoVo	LnCAP	PC3	T47D	A375	ASPC1	U87MG
2	H	0.031	0.353	0.124	0.60	0.108	0.42	0.062	2.16	21 (2)
8	Cl	1.73	0.030	0.012	−	0.048	0.030	1.58	0.427	24 (2)
14	OCH_3	0.011	0.004	0.004	0.005	0.010	0.033	0.004	0.355	> 100
15	CH_3	0.008	0.029	0.019	0.001	0.012	0.042	0.015	4.450	> 100
16	Br	1.48	0.006	0.006	0.002	0.018	0.037	0.006	0.331	> 100
17	F	4.87	0.010 (2)	0.017 (2)	0.009	0.027 (2)	0.032	0.007	0.592	13 (2)
20	CF_3	2.50	0.031	0.028	0.255	0.021	0.44	0.035	0.290	> 100

[a] HUVEC proliferation was induced by stimulation with LSGS and quantitated by measuring BrdU incorporation. The IC_{50} values were determined using GraphPad Prism software, and 95% confidence intervals for all data were in ranges of less than 2-fold of the reported values. The data were obtained using six serial dilutions of each compound with eight replications for each concentration. [b] The effects of compounds on tumor cells in log phase growth were measured by [^{14}C]-thymidine incorporation. The IC_{50} values were determined using GraphPad Prism software, and 95% confidence intervals for all data were in ranges of less than 2-fold of the reported values. The data were obtained in duplicate measurements at eight serial dilutions of each compound.

and Fyn (IC_{50} = 0.378 μM). These kinases may have some relevance, but the broad, potent tumor cell activity observed makes them unlikely candidates as the primary mechanism of the antiproliferative activity.

The nature of the antiproliferative effect of **17** was assessed by a cell counting experiment using a trypan blue exclusion assay with the H460 human lung carcinoma cell line. Unlike the nonselective kinase inhibitor staurosporine and the mitosis inhibitor colchicine, after 24 h treatment **17** did not cause the cell number to drop below the original cell colony plating density until the concentration of **17** exceeded 1.0 μM. This demonstrates that the low nanomolar antiproliferative activity observed for **17** in tumor cell lines appears to be a cytostatic, not a cytotoxic, phenomena up to concentrations of 1.0 μM. In this experiment the cytotoxic threshold for the staurosporine control was apparent at concentrations of 0.01 μM and for the colchicine control at 0.1 μM.[31]

Binding Model. Compounds **1** and **2** were minimized in a homology model of the ATP binding site of the PDGF receptor tyrosine kinase based upon the published crystal structure of the VEGF receptor tyrosine kinase (PDB code: 1VR2).[34] The homology model of PDGFR-β kinase was constructed using the *Composer* module in Sybyl v6.7 (Tripos Inc., St. Louis, MO). The sequences of PDGFR-β kinase and VEGF-R2 kinase are 56% identical and a sequence alignment of these two proteins is included in Supporting Information. Compounds **1** and **2** were docked in the ATP binding site of the PDGFR-β kinase homology model using Glide v2.0 (Schrödinger LLC., Portland, OR). Some 5000 conformations were generated for each ligand by the Monte Carlo method, and the 30 best poses were kept for further scoring based on an E-model scoring function. The complexes were minimized using AMBER94 force field with coordinates of backbone atoms fixed.

From the start it was apparent that two equienergetic docking orientations were available for **1** (Figures 1a,b) and **2** (Figures 2a,b). This picture is further complicated by the presumed ability of the pyrazole heterocycle to exist in two tautomeric forms. However, in 1D proton, 2D ROESY, 2D [^{1}H]−[^{13}C] gradient-HMBC, and 2D [^{1}H]−[^{15}N] gradient HMBC NMR experiments on the related analog **17**, no evidence was found for the presence of the pyrazole N(2)H tautomer. There was a 3:1 doubling of the resonances for the pyrazole N(1)H and exocyclic −NH−, suggesting hindered rotation about the pyrazole−N(H)−phenyl dihedral and the presence of two rotomers of **17** on the NMR time scale.[35]

We present here a model that assumes the N(1)H tautomer is the bioactive form of the pyrazole ring for **1** and **2**. While this tautomer is the major form found in solution based upon our NMR study, this evidence does not definitively elucidate the bioactive tautomeric form bound to the protein. However, the N(1)H tautomer does allow the modeled compounds to maintain a complementary hydrogen bond donor−acceptor network with the 'hinge' region of the ATP binding pocket. In the docking orientation illustrated in Figures 1a and 2a for 1 and 2, respectively, the tricyclic pyrazole portion of both molecules are directed along the lipophillic channel occupied by the triphosphate moiety of ATP, an orientation similar to that observed for the BMS indenopyrazoles in a crystal complex with CDK 2.[33] With this orientation we postulate a H-bonding network between the Glu542 carbonyl and the pyrazole N(1)−H for **1** and **2**, a H-bond between the amide NH of Tyr543 and the pyrazole N(2) of **1** and **2**, and for **2** there is an additional H-bond between the aniline N−H and the carbonyl of Met544. The alternative docking for **1** and **2** envisions a 'Tarceva-like' orientation[36] of the 6,7-dimethoxy-2,4-dihydroindeno[1,2-*c*]pyrazole ring system with the 6,7-dimethoxy group directed toward the highly variable 'selectivity region' at the solvent interface. For compounds **1** and **2** the pyrazole N(1)−H is anchored by a H-bond with the carbonyl of Met544 and the pyrazole N(2) supplies an H-bond acceptor interaction with the amide N−H of Tyr543. For compound **2**, the additional aniline N−H can bind with the Glu542 carbonyl.

Conclusion

We have shown that a series of tricyclic pyrazoles with potent inhibition activity against the angiogenesis target PDGFR-β kinase can be optimized to enhance a cellular antiproliferative activity unrelated to the original target kinase. This was accomplished by following in parallel the structure−activity relationships for both

PDGFR-β kinase inhibition and cell antiproliferative activity with a panel of both 'normal' and tumor cells. From this series, compound **17** (JNJ 10198409) emerged based on the PDGFR-β kinase inhibition activity and selective tumor cell antiproliferative effect. A cell counting experiment demonstrates the tumor cell antiproliferative activity of **17** is cytostatic, not cytotoxic, in nature at concentrations up to 1.0 μM, well above the low nanomolar IC_{50} observed for the antiproliferative effect.[31] Both kinase and nonkinase biomolecular targets are under consideration as potential drivers of the antiproliferative activity, but the mechanism of action is still a subject of active investigation.

Characterization of **17** in our kinase selectivity screen demonstrates that this compound has activity against c-Abl kinase similar to that reported for STI-571. With a kinase inhibition profile similar to STI-571 combined with potent antiproliferative activity, **17** may represent an improved agent for the treatment of the current clinical indication for STI-571, chronic myelogenous leukemia (CML), and a potential therapeutic approach for patients with STI-571-resistant CML.[37] In a broader context, **17** represents a class of antitumor agents endowed with a dual mechanism of action: an antiangiogenic effect based upon the potent PDGFR-β kinase inhibition and a cytostatic effect, due to the potent, selective antiproliferative activity in human tumor cell lines. Further work describing the in vitro and in vivo activity of this dual mechanism agent will be reported in due course.

Experimental Section

High-resolution mass spectra were obtained with a Auto Spec Micromass; low resolution mass spectral analyses were performed with an Agilent 1100 Series LC/MS. The ^{1}H NMR used in this study was a 360 MHz Bruker AM 360WB. Two HPLC systems were used for product purity assessment; HPLC system 1: Hewlett-Packard model 1050 HPLC with a 3.3 mm × 50 mm Supelco 3 μm AZB + C18 column, eluting with a mobile phase gradient of 4: 96 acetonitrile: water (0.1% TFA) to 100: 0 acetonitrile:water (0.1% TFA) over 0.5 min at a flow rate of 1.2 mL: min for a total run time of 9.5 min; HPLC system 2: Hewlett-Packard model 1100 HPLC with a 4.4 mm × 30 mm Luna 3 μm C18(2)100R column, eluting with a mobile phase gradient of 4: 96 acetonitrile:water (0.1% TFA) to 100: 0 acetonitrile:water (0.1% TFA) over 0.5 min at a flow rate of 1.2 mL: min for a total run time of 9.5 min.

Preparation of Study Compounds: 3-Fluoro-*N*-(6,7-dimethoxy-2,4-dihydroindeno[1,2-*c*]pyrazol-3-yl)phenylamine (17). A mixture of 5,6-dimethoxyindan-1-one (3.0 g, 0.0154 mol) and 3-fluorophenyl isothiocyanate (2.4 g, 0.0157 mol) in THF (3.0 mL) was added to lithium hexamethyldisilane (15.4 mL, 0.0154 mol) dropwise at room temperature. The reaction mixture was stirred for 12 h. Hydrazine (0.75 mL, 0.0154 mol) and acetic acid (0.96 mL) were added to the reaction mixture, which was then heated at the reflux temperature for 24 h. The resulting mixture was added to water (30 mL) and then extracted with CH_2Cl_2 (3 × 30 mL). The organic layers were combined and washed sequentially with aqueous $NaHCO_3$ solution (30 mL), water (30 mL), and brine solution (30 mL), dried (Na_2SO_4), and solvent was removed in vaccuo. The residue was dissolved in ethyl acetate and decolorized with charcoal and recrystallized to give compound **17** (3.5 g, 0.0107 mol, 69%) as an off white solid; mp 171–173.5 °C MS: *m/z* 326 $(M + H)^+$; [^{1}H]-NMR (DMSO-d_6) δ: 3.40 (s, 2H), 3.80 (s, 3H), 3.81 (s, 3H), 6.48–6.55 (t,1H), 7.1–7.2 (m 5H), 7.3–7.4 (d, 1H), 8.8 (s, 1H); HPLC purity (retention time): >99% (4.1 min); Calcd for $C_{18}H_{16}FN_3O_2$: C, 66.45; H, 4.96; N, 12.92: Found: C, 66.19; H, 4.76; N, 12.79.

Compounds **2**–**16** and **18**–**21** were prepared by essentially the same procedure from the appropriate starting materials. The starting materials, method of purification, spectral data, and analytical data are listed below:

(6,7-Dimethoxy-2,4-dihydroindeno[1,2-*c*]pyrazol-3-yl)-phenylamine, Trifluoroacetate Salt (2). This material was prepared by the method described for **17** starting from 5,6-dimethoxyindan-1-one and phenyl isothiocyanate. The desired product was isolated by reverse phase hplc using a C18 column and eluting with a gradient of CH_3CN/H_2O with 0.05% TFA to yield a solid: MS *m/z* 308 $(M^+ + H)$; [^{1}H]-NMR(DMSO-d_6) δ: 3.40 (2H, s, CH_2), 3.80 (3H, s, CH_3), 3.85 (3H, s, CH_3), 6.75 (1H, t, CH), 7.10–7.30 (6H, m, CH), 8.35 (1H, s, NH), 12.0 (1H, s, NH); HPLC purity: system 1, >99%, retention time: 4.0 min; system 2, 97.2% (214 nm) and 97.2% (254 nm), retention time: 4.40 min; HRMS calcd for $C_{18}H_{17}N_3O_2(M^+ + H)$ 308.139902, found 308.138883.

(2,4-Dihydroindeno[1,2-*c*]pyrazol-3-yl)phenylamine (3). This material was prepared by the method described for **17** starting from indan-1-one and phenyl isothiocyanate. The product was isolated by silica gel chromatography with 2% methanol:methylene chloride. Compound **3** was subsequently crystallized from methylcyclohexane:toluene as a white solid. mp 148–149 °C; MS *m/z* 248 $(M + H)^+$; [^{1}H]-NMR (DMSO-d_6) δ: 3.5 (s, 2H), 6.75 (t, 1H), 7.0–7.3 (m, 5H), 7.35 (t, 1H), 7.5 (dd, 2H), 8.4 (s, 1H), and 12.3 ppm (s, 1H); HPLC purity: system 2, 98.9% (214 nm) and 97.2% (254 nm), retention time: 4.70 min; HRMS calcd for $C_{16}H_{13}N_3$ $(M^+ + H)$ 248.118773, found 248.118420.

(7-Methoxy-2,4-dihydroindeno[1,2-*c*]pyrazol-3-yl)phenylamine, Trifluoroacetate Salt (4). This material was prepared by the method described for **17** starting from 6-methoxyindan-1-one and phenyl isothiocyanate. The target compound was purified by reverse phase HPLC with a C18 column and eluted with a gradient of CH_3CN/H_2O with 0.05% TFA to give a TFA salt: MS *m/z* 278 $(M^+ + H)$; [^{1}H]-NMR (DMSO-d_6) δ: 3.30 (s, 2H), 3.71 (s, 3H), 6.79 (m, 2H), 7.14 (m, 5H), 7.34 (d, 1H); HPLC purity: system 1, >99%, retention time: 4.5 min; system 2, 98.0% (214 nm) and 98.0% (254 nm), retention time: 4.84 min; HRMS calcd for $C_{17}H_{15}N_3O$ $(M^+ + H)$ 278.12337, found 278.128760.

(6-Methoxy-2,4-dihydroindeno[1,2-*c*]pyrazol-3-yl)phenylamine, (5). This material was prepared by the method described for **17** starting from 5-methoxyindan-1-one and phenyl isothiocyanate. MS *m/z* 278 $(M^+ + H)$; [^{1}H]-NMR (DMSO-*d6*) δ: 3.32 (br. s, 2H), 2.79 (s, 3H), 6.69–6.89 (m, 1H), 6.91–6.92 (d, 1H), 7.14–7.19 (m, 5H), 7.42–7.45 (d, 1H), 8.35 (br s, 1H); HPLC purity: system 1, >99%, retention time: 4.4 min; system 2, 97.6% (214 nm) and 97.8% (254 nm), retention time: 4.62 min; HRMS calcd for $C_{17}H_{15}N_3O$ $(M^+ + H)$ 278.129337, found 278.128924.

(5-Methoxy-2,4-dihydroindeno[1,2-*c*]pyrazol-3-yl)phenylamine, Trifluoroacetate Salt (6). This material was prepared by the method described for **17** starting from 4-methoxyindan-1-one and phenyl isothiocyanate. The crude mixture was purified to give **6** by reverse phase hplc and eluted from a C18 column with a gradient of CH_3CN/H_2O with 0.05% TFA to give a TFA salt: MS *m/z* 278 $(M^+ + H)$; [^{1}H]-NMR (DMSO-d_6) δ: 3.35 (s, 2H), 3.82 (s, 3H), 6.72 (t, 1H), 6.94 (d, 1H), 7.20 (m, 5H), 7.34 (t, 1H); HPLC purity: system 1, >99%, retention time: 4.6 min; system 2, 98.0% (214 nm) and 98.6% (254 nm), retention time: 4.80 min; HRMS calcd for $C_{17}H_{15}N_3O$ $(M^+ + H)$ 278.129337, found 278.129477.

2-Chloro-*N*-(6,7-dimethoxy-2,4-dihydroindeno[1,2-*c*]-pyrazol-3-yl)phenylamine, Trifluoroacetate Salt (7). This material was prepared by the method described for **17** starting from 5,6-dimethoxyindan-1-one and 2-chlorophenyl isothiocyanate. Elution of the crude material with reverse phase hplc using a C18 column and a gradient of CH_3CN/H_2O with 0.05% TFA gave pure **7** as a solid: MS *m/z* 341 $(M^+ + H)$; [^{1}H]-NMR (DMSO-d_6) δ: 3.40 (2H, s, CH_2), 3.80 (3H, s, CH_3), 3.85 (3H, s, CH_3), 6.90 (1H, t, CH), 7.10–7.30 (4H, m, CH), 7.40 (1H, d, CH), 7.90 (1H, s, NH); HPLC purity: system 1, >99%, retention time: 4.5 min; system 2, 98.8% (214 nm) and 98.9%

(254 nm), retention time: 4.82 min; HRMS calcd $C_{18}H_{16}ClN_3O_2$ (M^+ + H) 342.100930, found 342.101458.

3-Chloro-*N*-(6,7-dimethoxy-2,4-dihydroindeno[1,2-*c*]pyrazol-3-yl)phenylamine, Trifluoroacetate Salt (8). This material was prepared by the method described for **17** starting from 5,6-dimethoxyindan-1-one and 3-chlorophenyl isothiocyanate. The product was purified further by reverse phase HPLC with a C18 column eluted with a gradient of CH_3CN/H_2O with 0.05% TFA to yield **8** as a fluffy white solid: MS *m/z* 341 (M^+ + H); [^{1}H]-NMR (DMSO-d_6) δ: 3.40 (2H, s, CH_2), 3.80 (3H, s, CH_3), 3.85 (3H, s, CH_3), 6.80 (1H, d, CH), 7.10–7.25 (4H, m, CH), 7.40 (1H, s, CH), 8.80 (1H, s, NH); HPLC purity: system 1, >99%, retention time: 4.7 min; system 2, 100% (214 nm) and 100% (254 nm), retention time: 4.97 min; HRMS calcd $C_{18}H_{16}ClN_3O_2$ (M^+ + H) 342.100930, found 342.100880.

4-Chloro-*N*-(6,7-dimethoxy-2,4-dihydroindeno[1,2-*c*]pyrazol-3-yl)phenylamine, Hydrochloride Salt (9). This material was prepared by the method described for **17** starting from 5,6-dimethoxyindan-1-one and 4-chlorophenyl isothiocyanate. The product was purified by reverse phase HPLC with a C18 column and eluted with a gradient of CH_3CN/H_2O with 0.05% TFA. Compound **9** was a white solid: MS *m/z* 341 (M^+ + H)$^+$; [^{1}H]-NMR (DMSO-d_6) δ: 3.50 (2H, s, CH_2), 3.80 (6H, s, CH_3), 7.30 (2H, d, CH), 7.30 (1H, s, CH), 7.35 (1H, s, CH), 7.40 (2H, d, CH); HPLC purity: system 1, >99%, retention time: 4.6 min; system 2, 99.0% (214 nm) and 99.7% (254 nm), retention time: 4.93 min; HRMS calcd $C_{18}H_{16}ClN_3O_2$ (M^+ + H) 342.100930, found 342.101085.

2,5-Dichloro-*N*-(6,7-dimethoxy-2,4-dihydroindeno[1,2-*c*]pyrazol-3-yl)phenylamine, Trifluoroacetate Salt (10). This material was prepared by the method described for **17** starting from 5,6-dimethoxyindan-1-one and 2,5-dichlorophenyl isothiocyanate. Compound **10** was isolated by reverse phase HPLC with a C18 column eluting with a gradient of CH_3CN/H_2O with 0.05% TFA to give a TFA salt: MS *m/z* 375 (M^+ + H); [^{1}H]-NMR (DMSO-d_6) δ: 3.45 (2H, s, CH_2), 3.80 (3H, s, CH_3), 3.85 (3H, s, CH_3), 6.85 (1H, d, CH), 7.20 (1H, s, CH), 7.25 (1H, s, CH), 7.40 (1H, d, CH), 7.45 (1H, s, NH), 8.00 (1H, s, CH); HPLC purity: system 1, >99%, retention time: 5.4 min; system 2, 100% (214 nm) and 98.4% (254 nm), retention time: 5.64 min; HRMS calcd for $C_{18}H_{15}Cl_2N_3O_2$ (M^+ + H) 376.061957, found 376.060153.

2,4-Dichloro-*N*-(6,7-dimethoxy-2,4-dihydroindeno[1,2-*c*]pyrazol-3-yl)phenylamine, Trifluoroacetate Salt (11). This material was prepared by the method described for **17** starting from 5,6-dimethoxyindan-1-one and 2,4-dichlorophenyl isothiocyanate. Crude **11** was further purified by reverse phase HPLC by eluting from a C18 column with a gradient of CH_3CN/H_2O with 0.05% TFA to give pure **11** as a TFA salt: MS *m/z* 375 (M^+ + H); [^{1}H]-NMR (DMSO-d_6) δ: 3.41 (s, 2H), 3.80 (s, 3H), 3.81 (s, 3H), 7.25 (s, 1H), 7.35 (s, 1H), 7.40 (d, 2H), 7.65 (d, 1H); HPLC purity: system 1, >99%, retention time: 5.5 min; system 2, 100% (214 nm) and 99.8% (254 nm), retention time: 5.25 min; HRMS calcd for $C_{18}H_{15}Cl_2N_3O_2$ (M^+ + H) 376.061957, found 376.060828.

3,4-Dichloro-*N*-(6,7-dimethoxy-2,4-dihydroindeno[1,2-*c*]pyrazol-3-yl)phenylamine, Hydrochloride Salt (12). This material was prepared by the method described for **17** starting from 5,6-dimethoxyindan-1-one and 3,4-dichlorophenyl isothiocyanate. The crude was treated with saturated HCl in ether solution to yield hydrochloride salt: MS *m/z* 375 (M^+ + H); [^{1}H]-NMR (DMSO-d_6) δ: 3.41 (s, 2H), 3.81 (s, 6H), 7.18 (m, 3H), 7.49 (d, 1H), 7.61 (s, 1H); HPLC purity: system 1, >99%, retention time: 5.3 min; system 2, 99% (214 nm) and 99.4% (254 nm), retention time: 5.49 min; HRMS calcd for $C_{18}H_{15}Cl_2N_3O_2$ (M^+ + H) 376.061957, found 376.060461.

3,5-Dichloro-*N*-(6,7-dimethoxy-2,4-dihydroindeno[1,2-*c*]pyrazol-3-yl)phenylamine, Hydrochloride Salt (13). This material was prepared by the method described for **17** starting from 5,6-dimethoxyindan-1-one and 3,5-dichlorphenyl isothiocyanate. The crude material was recrystallized from ethanol. The first and second crops of solid were combined and dissolved in hot CH_3CN, to which an equal volume of HCl-ether solution was added to precipitate the compound **13**, which was collected and dried under vacuum at 60 °C. mp > 270 °C; MS *m/z* 376 and 378 (M^+ + H); [^{1}H]-NMR (DMSO-d_6) δ: 3.44 (s, 2H), 3.83 (s, 3H), 3.82 (s, 3H),6.93 (s, 1H),7.19 (s, 1H), 7.21 (s, 1H), 7.35 (s, 2H); HPLC purity: system 1, >99%, retention time: 5.7 min; system 2, 96.8% (214 nm) and 99.6% (254 nm), retention time: 5.83 min; HRMS calcd for $C_{18}H_{15}Cl_2N_3O_2$ (M^+ + H) 376.061957, found 376.061027.

3-Methoxy-*N*-(6,7-dimethoxy-2,4-dihydroindeno[1,2-*c*]pyrazol-3-yl)phenylamine, Hydrochloride Salt (14). This material was prepared by the method described for **17** starting from 5,6-dimethoxyindan-1-one and 3-methoxyphenyl isothiocyanate. The crude was treated with saturated hydrochloric acid in ether solution to yield an off white solid: MS *m/z* 338 (M^+ + H); [^{1}H]-NMR (DMSO-d_6) δ: 3.46 (s, 2H), 3.74 (s, 3H), 3.81 (s, 3H), 3.82 (s, 3H), 6.50–6.52 (d, 1H), 6.75–6.77 (d, 1H), 6.77 (s, 1H), 7.17–7.27 (m, 3H); HPLC purity: system 2, 100% (214 nm) and 100% (254 nm), retention time: 4.52 min; HRMS calcd for $C_{19}H_{19}N_3O_3$ (M^+ + H) 338.150467, found 338.149426.

3-Methyl-*N*-(6,7-dimethoxy-2,4-dihydroindeno[1,2-*c*]pyrazol-3-yl)phenylamine, (15). This material was prepared by the method described for **17** starting from 5,6-dimethoxyindan-1-one and 3-methylphenyl isothiocyanate. The crude material was recrystallized in ethyl acetate and decolorized with charcoal to yield **15** as an off white solid: MS *m/z* 322 (M^+ + H); [^{1}H]-NMR (DMSO-d_6) δ: 2.24 (s, 3H), 3.78 (s, 3H), 3.82 (s, 3H), 6.54–6.56 (d, 1H), 7.04–7.19 (m, 5H), 8.24 (br s, 1H); HPLC purity: system 1, >99%, retention time: 4.3 min; system 2, 99.0% (214 nm) and 99.2% (254 nm), retention time: 4.72 min; HRMS calcd for $C_{19}H_{19}N_3O_2$ (M^+ + H) 322.155552, found 322.154514.

3-Bromo-*N*-(6,7-dimethoxy-2,4-dihydroindeno[1,2-*c*]pyrazol-3-yl)phenylamine, Trifluoroacetate Salt (16). This material was prepared by the method described for **17** starting from 5,6-dimethoxyindan-1-one and 3-bromophenyl isothiocyanate. Compound **16** was purified by reverse phase HPLC with a C18 column eluted with a gradient of CH_3CN/H_2O with 0.05% TFA to give a TFA salt; MS *m/z* 385 (M^+ + H); [^{1}H]-NMR (DMSO-d_6) δ: 3.41 (s, 2H), 3.77 (s, 3H), 3.79 (s, 3H), 6.90 (dd, 1H), 7.14 (m, 3H), 7.22 (s, 1H), 7.49 (s, 1H), 8.81 (br s, 1H); HPLC purity: system 1, >99%, retention time: 4.8 min; system 2, 100% (214 nm) and 99.7% (254 nm), retention time: 5.06 min; HRMS calcd for $C_{18}H_{16}BrN_3O_2$ (M^+ + H) 386.050413, found 386.048508.

3-Cyano-*N*-(6,7-dimethoxy-2,4-dihydroindeno[1,2-*c*]pyrazol-3-yl)phenylamine, Trifluoroacetate Salt (18). This material was prepared by the method described for **17** starting from 5,6-dimethoxyindan-1-one and 3-cyanophenyl isothiocyanate. Reverse phase HPLC was used to further purify **18** by elution from a C18 column with a gradient of CH_3CN/H_2O with 0.05% TFA to give the TFA salt of the product as a fluffy white solid: MS *m/z* 333 (M + H)$^+$; [^{1}H]-NMR (DMSO-d_6) δ: 3.45 (2H, s, CH_2), 3.80 (3H, s, CH_3), 3.85 (3H, s, CH_3), 7.15 (1H, s, CH), 7.20 (1H, d, CH), 7.25 (1H, s, CH), 7.40 (1H, t, CH), 7.50 (1H, d, CH), 7.80 (1H, s, CH), 9.00 (1H, s, NH); HPLC purity: system 1, >99%, retention time: 4.2 min; system 2, 95.6% (214 nm) and 97.7% (254 nm), retention time: 5.54 min; HRMS calcd for $C_{19}H_{16}N_4O_2$ (M^+ + H) 333.135151, found 333.134670.

3-Carbomethoxy-*N*-(6,7-dimethoxy-2,4-dihydroindeno-[1,2-*c*]pyrazol-3-yl)phenylamine, (19). This material was prepared by the method described for **17** starting from 5,6-dimethoxyindan-1-one and 3-carbomethoxyphenyl isothiocyanate. The crude was recrystallized in ethyl acetate to give a light brown solid: MS *m/z* 366 (M + H)$^+$; [^{1}H]-NMR (DMSO-d_6) δ: 3.40 (s, 2H), 3.79 (s, 3H), 3.83 (s, 3H), 3.83 (s, 3H), 7.13 (s, 1H), 7.21 (s, 1H), 7.32 (br s, 1H), 7.34 (br s, 1H), 8.68 (br s, 1H); HPLC purity: system 1, >99% retention time: 4.2 min; system 2, 99.0% (214 nm) and 98.4% (254 nm), retention time: 4.56 min; HRMS calcd for $C_{20}H_{19}N_3O_4$ (M^+ + H) 366.145381, found 366.144026.

3-Trifluoromethyl-*N*-(6,7-dimethoxy-2,4-dihydroindeno-[1,2-*c*]pyrazol-3-yl)phenylamine, Trifluoroacetate Salt (20). This material was prepared by the method described for

17 starting from 5,6-dimethoxyindan-1-one and 3-trifluoromethylphenyl isothiocyanate. Compound **20** was further purified by a reverse phase HPLC fitted a C18 column and eluted with a gradient of CH_3CN/H_2O with 0.05% TFA to yield the trifluoroacetate salt as a fluffy white solid: MS *m/z* 376 (M^+ + H); [^{1}H]-NMR (DMSO-d_6) δ: 3.42 (s, 2H), 3.78 (s, 3H), 3.80 (s, 3H), 7.05 (d, 1H0, 7.17 (s, 1H), 7.22 (s, 1H), 7.40 (m, 2H), 7.68 (s, 1H), 8.92 (br s, 1H); HPLC purity: system 1, >99%, retention time: 5.2 min; system 2, 98.4% (214 nm) and 99.4% (254 nm), retention time: 5.25 min; HRMS calcd for $C_{19}H_{16}F_3N_3O_3$ (M^+ + H) 376.127287, found 376.125758.

3-Carboxy-*N*-(6,7-dimethoxy-2,4-dihydroindeno[1,2-*c*]-pyrazol-3-yl)phenylamine, Trifluoroacetate Salt (21). To a flask under argon was added 0.16 g (0.33 mmol) of compound **19**, 4.5 mL of THF, 1 mL of H_2O, and 0.043 g (1.0 mmol) of lithium hydroxide monohydrate. The reaction mixture was stirred at room temperature for 2 days. The solvent was evaporated, and then water and a drop of TFA were added. This material was purified by reverse phase HPLC with a C18 column and eluted with a gradient of CH_3CN/H_2O with 0.05% TFA to give 0.06 g (39%) of **21** as a TFA salt: MS *m/z* 352 (M^+ + H); [^{1}H]-NMR (DMSO-d_6) δ : 3.4 (s, 2H), 3.8−3.9 (2s, 6H), 7.1 (s, 1H), 7.2 (s, 1H), 7.3−7.5 (m, 2H), 7.8 (s, 1H), 8.8 (bs, 1H); HPLC purity: system 1, >99%; system 2, 100% (214 nm) and 86.5% (254 nm), retention time: 3.96 min; HRMS calcd for $C_{19}H_{17}N_3O_4$ (M^+ + H) 352.129731, found 352.128941.

Inhibition of PDGF-Receptor Kinase Activity. PDGF-R kinase activity was assayed by the ability of the kinase to phosphorylate a consensus sequence of its target proteins, PLCγ in a cell-free system, in particular, a PLC1 peptide comprising the tyrosine residue where the phosphorylation occurs was used for the assay.

The following reagents were prepared for the assay:

10× Kinase Buffer (500 mM Tris-HCl pH = 8, 100 mM $MgCl_2$, 1 mM Na_3VO_4); 10 mM DTT (final concentration at 1 mM in assay); 10 mM ATP (final concentration at 5 μM in assay); [^{33}P]-γ-ATP (Cat. No.: NEG/602H. 2000-3000 Ci/mmol) purchased from NEN; purified, soluble, recombinant PDGF-receptor beta enzyme comprising the tyrosine kinase domain (from amino acid 545 to 1106 of GenBank Access NO: AAA36427) at 0.4 mg/mL; enzyme dilution buffer (50 mM Tris-HCl pH = 8.0, 0.1% BSA); wash/stop buffer (PBS +100 mM EDTA); NEN Streptavidin Flashplate (cat#: SMP-103) which binds to the biotinylated PLC1 peptide but not the PDGF-R enzyme; PLC1 peptide (Biotin-KHKKLAEGSAYEEV−Amide) at 1 mM in 50 mM Tris-HCL with pH of 8.0.

Reagents were first mixed according to the following regimen: 1100 μL of 10× Kinase Buffer, 1100 μL of 10 mM DTT, 5.5 μL of 10 mM cold ATP, 2.75 μL of 1 mM PLC1 Peptide 8.8 μL of [^{33}P]-γ-ATP (10 mCi/ml), and 5475 μL of H_2O. The above mixture was dispensed into each well of a Flashplate at 70 μL/well. To test the effect of a compound on PDGF-R kinase activity, the test compound either in a fixed concentration or in serially diluted concentrations in 100% DMSO was added to appropriate wells at 1 μL/well. Enzyme PDGF-R was diluted in enzyme dilution buffer. The kinase reaction was initiated by adding 30 μL of diluted PDGF-R enzyme solution to each well on the Flashplate containing radioactive ATP and PLC1, except wells of column 12 rows E through H, which were used to calculate the plate background. The Flashplate was swirled to mix and was incubated at 30 °C for 60 min. Then, the reaction mixture was decanted and the Flashplate was washed three times each with 200 μL of wash/stop buffer. Subsequently, each well on the Flashplate was filled with 200 μL of wash/stop buffer. The amount of [^{33}P] retained in each well was measured using a Packard TopCount after the plate was sealed with a transparent plate sealer. When a test compound inhibited the PDGF-R kinase activity, the well containing such a compound contained less [^{33}P] as compared to the well without the compound. The percentage of inhibition of the test compound on PDGF-R kinase activity is defined as the amount of [^{33}P] retained in the well containing the compound divided by the amount of [^{33}P] in the well without the compound. To test the potency of inhibition of present compounds, an IC_{50} for an individual compound was measured using the above procedure. The IC_{50} for PDGF-R kinase activity refers to the concentration of an inhibitor at which the activity of the PDGF-R kinase is reduced by one-half as compared with reactions containing no inhibitor.

Table 4. Kinase Panel Inhibition Data for **17**

kinase	IC_{50} (μM)
PDGFR-β	0.0042
PDGFR-α	0.045
VEGFR	3.1
HER-2	>10
EGFR	>100
bFGFR1	45.8
c-ABL	0.022
CDK1	>100
CDK2	>10
CDK4	>100
CDK7	56.7
c-SRC	0.185
LCK	0.100
FYN	0.378
PKA	>100
GSK3	13
MAPK	>100
IRK	>100
FAK	>100
Casein K1	7.2
Casein K2	>100
Calmodulin K	>10

Kinase Selectivity. Assays and Substrates. Selectivity versus additional kinases (Table 4) was assessed using in-house assays as described above for the PDGFR kinase assay but incorporating appropriate modifications to the assay buffer and substrates for each respective kinase enzyme.[38] Compounds were further evaluated for kinase selectivity in the Upstate panel of kinases (Upstate, L.L.C., Charlottesville, VA).

Cell Proliferation Assay in Normal Cells in the Presence of PDGF Stimulation. The effect of compounds on cell proliferation in normal human primary cells, in particular, cryopreserved human coronary artery smooth muscle cells (HCASMC), in the presence of PDGF stimulation was tested based on incorporation of [^{14}C]-thymidine into DNA of cells.

The following materials were purchased from their respective sources:

Recombinant human PDGF beta homodimer, rhPDGF-BB purchased from R&D System (Minneapolis, MN, Cat. No: 220-BB); cryopreserved human coronary artery smooth muscle cells (HCASMC), tissue culture medium for HCASMC, and smooth muscle growth supplement (SMGS) purchased from Cascade Biologics (Portland, OR, HCASMC Cat. No: C-017−5C; Medium 231 Cat. No: M-231−500; and SMGS Cat. No: S-007−25); 96-well CytoStar tissue culture treated scintillating microplates purchased from Amersham (Piscataway, NJ, Cat. No: RPNQ0160); methyl ^{14}C-thymidine at 56 mCi/mmol (250 μCi/2.5 mL) purchased from NEN (Cat. No.: NEC568); DMSO from Sigma (St. Louis, MO, Cat. No: D-5879); sterile reagent reservoirs from Costar (VWR International, Inc., West Chester, PA, Cat. No: 4870); Dulbecco's PBS from Gibco (Cat. No: 14190−136); backing tape white plate cover for bottom of CytoStar plate from Packard (Cat. No: 6005199).

HCASMC were seeded at approximately 4000 cells/well in a volume of 100 μL of complete Medium 231 with SMGS. Cells were grown for 48 h until they reached approximately 80% confluence. They were rendered quiescent by incubation in SMGS-free Medium 231 for 24 h. Cell culture media was replenished with SMGS-free Medium 231 containing rhPDGF-BB at 50 ng/mL in a total volume of 100 μL/well, and 1 μL of test compounds in serially diluted concentrations in 100% DMSO was added to each well. For the maximum growth control wells, only 1 μL of 100% DMSO was added; for minimum growth (blank) wells, 1 μL of 10 mM cycloheximide was added to each well. After incubation for 24 h, 20 μL of [^{14}C]-thymidine mix was added to each well and the [^{14}C]-thymidine mix was made according to the following regimen: 220 μL of [^{14}C]-thymidine, 1980 μL of SMGS-free Medium 231. Cells were incubated for an additional 24 h in media containing test compounds, rhPDGF-BB and [^{14}C]-thymidine. Then, the reaction mixture was discarded and the plate was washed three times each with 200 μL of PBS. Subsequently, each well on the plate was filled with 200 μL of PBS. The top of the plate was sealed with transparent plate sealer, and white plate backing sealers were applied to the bottom of plates. The retained [^{14}C] inside each well was measured using a Packard Top Count. The amount of [^{14}C] retained in a well correlates to the proliferation of cells inside the well. When a test compound inhibited rhPDGF-BB-induced HCASMC proliferation, the well containing such a compound retained less [^{14}C] as compared to the maximum growth control wells without the compound. To test the potency of inhibition, the IC_{50} of an individual compound on the inhibition of rhPDGF-BB-induced HCASMC proliferation was measured using the above procedure. The IC_{50} refers to the concentration of the test compound at which the amount of rhPDGF-BB-induced HCASMC proliferation is reduced by one-half as compared to the maximum growth control wells without the compound.

Cell Proliferation Assay in Normal Cells in the Absence of PDGF Stimulation. Human umbilical vein endothelial cells (HUVEC) were purchased from Cascade Biologics. For propagation, HUVEC cells were grown in M-200 media supplemented with LSGS − *L*ow *S*erum *G*rowth *S*upplement (Cascade Biologics). For studies, cells were detached with a trypsin/EDTA solution and washed three times with 10 mL of F12K (LS, low serum) media and then centrifuged at 400*g* for 5 min. F-12K (LS) media is F-12K media containing 0.2% heat-treated fetal bovine serum. Cell concentrations were adjusted to 5×10^4cells/mL in F-12K (LS) media and 200 μL (1×10^4 cells) were added to each well of a 96-well plate. Cells were then incubated for 16 to 20 h at 37 °C under 95% air/5% CO_2 to allow time for the cells to attach and become quiescent. Cell proliferation was stimulated by adding 50 μL of a 1:10 dilution of LSGS in F12K (LS). Maximum-stimulated control wells were prepared by adding 50 μL of a 1:10 dilution of LSGS, and 50 μL of F-12K (LS) media was added to negative controls. Compounds for testing are added at a volume of 2.5 μL to achieve the desired final drug concentrations of 10 μM, 1 μM, 0.1 μM, 0.01 μM, and 0.001 μM. Replicates of eight wells per condition were included. Cells were incubated at 37 °C overnight. On the next day, 25 μL of BrdU (1:100 dilution of stock in F-12K (LS) media was added to each well. Cells were incubated for an additional 20−24 h. All reagents for development were purchased from Roche (cat# 1 647 229). After the addition of substrate solution and a 30−40 min incubation, plates were read at 405 nm on a 96-well plate reader. IC_{50} values were determined using GraphPad Prism software.

Cell Proliferation Assay in Tumor Cell Lines. AsPC-1, PC3, H460, LoVo, A375, LnCAP, U87MG, and T47D cells were purchased from ATCC and grown in the recommended media type for each cell line. Cell proliferation assays were performed by trypsinizing the cells and seeding them to 96-well Cytostar tissue culture treated scintillating microplates (Amersham).[38] Cell concentrations were from 3×10^3 to 7×10^3 cells per well in a volume of 100 μL of complete media. Cells were allowed to adhere and grow for 24 h in a 37 °C, 5% CO_2 incubator. Ten-fold dilutions of compounds in 100% DMSO were added to the cells for final concentrations ranging from 100 μM to 0.1 nM. Each compound concentration was run in duplicate, and the final concentration of DMSO in the cell culture did not exceed 1%. Following the addition of drug, cells were incubated for an additional 24 h. Methyl [^{14}C] thymidine (Perkin-Elmer) was then added to the cells at a specific activity of 0.1 μCi per well, followed by a final 24-h incubation. Plates were then washed twice with PBS at a volume of 200 μL per well. After the final wash, each well was filled with 200 μL of PBS and sealed. Plates were read on a Top Count instrument (Perkin-Elmer). IC_{50} values were determined using GraphPad Prism software.

Supporting Information Available: Detailed experimental procedures and spectra are provided for the NMR experiments described for **17**. The sequence alignment used to develop the homology model of the PDGF RTK ATP binding site is also included. This material is available free of charge via the Internet at http://pubs.acs.org.

References

(1) Folkman, J. Angiogenesis in Cancer, Vascular, Rheumatoid and Other Diseases. *Nature Med.* **1995**, *1*, 27−31.
(2) Folkman, J. Anti-angiogenesis: New Concept for Therapy of Solid Tumors. *Ann. Surg.* **1972**, *175*, 409−416.
(3) Folkman, J. Clinical Implications of Research on Angiogenesis. *N. Engl. J. Med.* **1995**, *333*, 1757−1763.
(4) Gale, N. W.; Yancopoulos, G. D. Growth Factors Acting via Endothelial Cell-Specific Receptor Tyrosine Kinases: VEGFs, Angiopoietins and Ephrins in Vascular Development. *Genes Dev*. **1999**, *13*, 1055−1066.
(5) Battegay, E. J.; Rupp, J.; Iruela-Arispe, L.; Sage, E. H.; Pech, M. PDGF-BB Modulates Endothelial Proliferation and Angiogenesis In Vitro via PDGF-β Receptors. *J. Cell Biol.* **1994**, *125*, 917−928.
(6) Thommen, R.; Humar, R.; Misevic, G.; Pepper, M. S.; Hahn, A. W. A.; John, M.; Battegay, E. J. PDGF-BB Increases Endothelial Migration on Cord Movements During Angiogenesis In Vitro. *J. Cell Biochem.* **1997**, *64*, 403−413.
(7) Sato, N.; Beitz, J. G.; Kato, J.; Yamamoto, M.; Clark, J. W.; Calabresi, P.; Frackelton, A. Platelet-Derived Growth Factor Indirectly Stimulates Angiogenesis In Vitro. *Am. J. Pathol*. **1993**, *142*, 1119−113.
(8) Kumar, R.; Yoneda, J.; Bucana, C. D.; Fidler, I. J. Regulation of Distinct Steps of Angiogenesis by Different Angiogenic Molecules. *Int. J. Oncol.* **1998**, *12*, 749−757.
(9) Sundberg, C.; Lungstrom, M.; Lindmark, G.; Gerdin, B.; Rubin, K. Microvascular Pericytes Express Platelet-Derived Growth Factor-β Receptors in Human Healing Wounds and Colorectal Adenocarcinoma. *Am. J. Pathol.* **1993**, *143*, 1377−1388.
(10) Antoniades, H. N.; Galanopoulos, T.; Neville-Golden, J.; O'Hara, C. J. Malignant Epithelial Cells in Primary Human Lung Carcinomas Coexpress In Vivo Platelet-Derived Growth Factor (PDGF) and PDGF Receptor mRNAs and Their Protein Products. *Proc. Natl. Acad. Sci., U.S.A.* **1993**, *89*, 3942−3946.
(11) Seymour, L.; Dajee, D.; Bezwoda, W. R. Tissue Platelet-Derived Growth Factor (PDGF) Predicts for Shortened Survival and Treatment Failure in Advanced Breast Cancer. *Breast Cancer Res. Treat.* **1993**, *26*, 247−252.
(12) Lindmark, G.; Sundberg, C.; Glimelius, B. L.; Rubin, K.; Gerdin, B. Stromal Expression of Platelet-Derived Growth Factor-β Receptor and Platelet-Derived Growth Factor B−Chain in Colorectal Cancer. *Lab. Invest*. **1993**, *69*, 682−689.
(13) Plate, K. H.; Breier, G.; Farrell, C. L.; Risau, W. Platelet-Derived Growth Factor Receptor-β Is Induced During Tumor Development and Upregulated During Tumor Progression in Endothelial Cells in Human Gliomas. *Lab. Invest.* **1992**, *67*, 529−534.
(14) Yosida, K.; Kuniyasu, H.; Yasui, W.; Kitadai, Y.; Toge, T.; Tahara, E. Expression of Growth Factors and Their Receptors in Human Esophageal Carcinomas: Regulation of Expression by Epidermal Growth Factor and Transforming Growth Factor-α. *J. Cancer Res. Clin. Oncol.* **1993**, *119*, 401−407.
(15) Ariad, A.; Seymour, L.; Bezwoda, W. R. Platelet-Derived Growth Factor (PDGF) in Plasma of Breast Cancer Patients: Correlation with Age and Rate of Progression. *Breast Cancer Res. Treat.* **1991**, *20*, 11−17.
(16) Anan, K.; Morisaki, T.; Katano, M.; Ikubo, A.; Kitsuki, H.; Uchiyama, A.; Kuroki, S.; Tanaka, M.; Torisu, M. Vascular Endothelial Growth Factor and Platelet-Derived growth Factor are Potential Angiogenic and Metastatic Factors in Human Breast Cancer. *Surgery* **1996**, *119*, 333−339.
(17) Bhardwaj, J. B.; Klassen, J.; Cossette, N.; Sterns, E.; Tuck, A.; Deeley, R.; Sengupta, S.; Elliott, B. Localization of Platelet-Derived Growth Factor-β Receptor Expression in the Periepithelial Stroma of Human Breast Carcinoma. *Clin. Cancer Res.* **1996**, *2*, 773−782.
(18) Heldin, C. H.; Ostman, A.; Ronnstrand, L. Signal Transduction via Platelet-Derived Growth Factor Receptors. *Biochim. Biophys. Acta* **1988**, *1378*, F79−F113.
(19) Kazlauskas, A.; Cooper, J. A. Autophosphorylation of the PDGF Receptor in the Kinase Insert Region Regulates Interactions with Cell Proteins. *Cell* **1989**, *58*, 1121−1133.
(20) Risau, W. Mechanisms of Angiogenesis. *Nature (London)* **1997**, *386*, 671−674.
(21) Lowenstein, E. J.; Daly, R. J.; Batzer, A. G.; Li, W.; Margolis, B.; Lammers, R.; Ullrich, A.; Skolnik, E. Y.; Bar-Sagi, D.; Schlessinger, J. The SH2 and SH3 Domain-Containing Protein GRB2 Links Receptor Tyrosine Kinases to Ras Signaling. *Cell* **1992**, *70*, 431−42.

(22) Ramakrishnan, V.; Escobedo, M. A.; Fretto, L. J.; Seroogy, J. J.; Tomlinson, J. E.; Wolf, D. L. A Novel Monoclonal Antibody Dependent on Domain 5 of the Platelet-Derived Growth Factor-β Receptor Inhibits Ligand Binding and Receptor Activation. *Growth Factors (Chur, Switzerland)* **1993**, *8*, 253−65.

(23) Engstrom, U.; Engstrom, A.; Ernlund, A.; Westermark, B.; Heldin, C. H. Identification of a Peptide Antagonist for Platelet-Derived Growth Factor. *J. Biol. Chem.* **1992**, *267*, 16581−16587.

(24) Brennand, D. M.; Dennehy, U.; Ellis, V.; Scully, M. F.; Tripathi, P.; Kakkar, V. V.; Patel, G. Identification of a Cyclic Peptide Inhibitor of Platelet-Derived Growth Factor-BB Receptor Binding and Mitogen-Induced DNA Synthesis in Human Fibroblasts. *FEBS Lett.* **1997**, *413*, 70−4.

(25) Klohs, W. D.; Fry, D. W.; Kraker, A. J. Inhibitors of Tyrosine Kinase. *Curr. Opin. Oncol.* **1997**, *9*, 562−568.

(26) Levitzki, A.; Gazit, A. Tyrosine Kinase Inhibition: an Approach to Drug Development. *Science* **1995**, *267*, 1782−1788.

(27) Shawver, L. K.; Lipson, K. E.; Fong, T.; Annie T.; McMahon, G.; Plowman, G. D.; Strawn, L. M. Receptor Tyrosine Kinases as Targets for Inhibition of Angiogenesis. *Drug Discovery Today* **1997**, *2*, 50−63.

(28) (a) Laird, A. D.; Vajkoczy, P.; Shawver, L. K.; Thurnher, A.; Liang, C.; Mohammadi, M.; Schlessinger, J.; Ulrich, A.; Hubbard, S. R.; Blake, R. A.; Fong, A. T.; Strawn, L. M.; Sun, L.; Tang, C.; Hawtin, R.; Tang, F.; Shemoy, N.; Hirth, K. P.; McMahon, G.; Cherrington, J. M. SU6668 is a Potent Anti-Angiogenic and Anti-tumor Agent that Induces Regression of Established Tumors. *Cancer Res*. **2000**, *60*, 4152−4160; (b) Myers, M. R.; He, W.; Hanney, B.; Setzer, N.; Maguire, M. P.; Zulli, A.; Bilder, G.; Galzcinski, H.; Amin, D.; Needle, S.; Spada, A. P. Potent Quinoxaline-Based Inhibitors of PDGF Receptor Tyrosine Kinase Activity. Part 1: SAR Exploration and Effective Bioisosteric Replacement of a Phenyl Substituent. *Bioorg. Med. Chem. Lett.* **2003**, *13*, 3091−3095; (c) He, W.; Myers, M. R.; Hanney, B.; Spada, A. P.; Bilder, G.; Galzcinski, H.; Amin, D.; Needle, S.; Page, K.; Jayyosi, Z.; Perrone, M. H. Potent Quinoxaline-Based Inhibitors of PDGF Receptor Tyrosine Kinase Activity. Part 2: The Synthesis and Biological Activities of RPR127963, an Orally Bioavailable Inhibitor. *Bioorg. Med. Chem. Lett.* **2003**, *13*, 3097−3100; (d) Manley, P. W.; Breitenstein, W.; Brueggen, J.; Cowan-Jacob, S. W.; Furet, P.; Mestan, J.; Meyer, T. Urea Derivatives of STI571 as Inhibitors of Bcr-Abl and PDGFR Kinases. *Bioorg. Med. Chem. Lett.* **2004**, *14*, 5793−5797; (e) Heath, J. A.; Mehrotra, M. M.; Chi, S.; Yu, J.-C.; Hutchaleelaha, A.; Hollenbach, S. J.; Giese, N. A.; Scarborough, R. M.; Pandey, A. Identification of 4-Piperazin-1-yl-quinazoline Template Based Aryl and Benzyl Thioureas as Potent, Selective, and Orally Bioavailable Inhibitors of Platelet-Derived Growth Factor (PDGF) Receptor. *Bioorg. Med. Chem. Lett.* **2004**, *14*, 4867−4872; (f) Kubo, K.; Ohyama, S.-I.; Shimizu, T.; Takami, A.; Murooka, H.; Nishitoba, T.; Kato, S.; Yagi, M.; Kobayashi, Y.; Iinuma, N.; Isoe, T.; Nakamura, K.; Iijima, H.; Osawa, T.; Izawa, T. Synthesis and Structure−Activity Relationship for New Series of 4-Phenoxyquinoline Derivatives as Specific Inhibitors of Platelet-Derived Growth Factor Receptor Tyrosine Kinase. *Bioorg. Med. Chem.* **2003**, *11*, 5117−5133; (g) Matsuno, K.; Ushiki, J.; Seishi, T.; Ichimura, M.; Giese, N. A.; Yu, J.-C.; Takahashi, S.; Oda, S.; Nomoto, Y. Potent and Selective Inhibitors of Platelet-Derived Growth Factor Receptor Phosphorylation. 3. Replacement of Quinazoline Moiety and Improvement of Metabolic Polymorphism of 4-[4-(N-Substituted (thio)carbamoyl)-1-piperazinyl]-6,7-dimethoxyquinazoline Derivatives. *J. Med. Chem.* **2003**, *46*, 4910−4925; (h) Matsuno, K.; Seishi, T.; Nakajima, T.; Ichimura, M.; Giese, N. A.; Yu, J.-C.; Oda, S.; Nomoto, Y. Potent and Selective Inhibitors of Platelet-Derived Growth Factor Receptor Phosphorylation. Part 4: Structure−Activity Relationships for Substituents on the Quinazoline Moiety of 4-[4-(N-Substituted-(thio)carbamoyl)-1-piperazinyl]-6,7-dimethoxyquinazoline Derivatives. *Bioorg. Med. Chem. Lett.* **2003**, *13*, 3001−3004; (i) Gazit, A.; Yee, K.; Uecker, A.; Bohmer, F.-D.; Sjoblom, T.; Ostman, A.; Waltenberger, J.; Golomb, G.; Banai, S.; Heinrich, M. C.; Levitzki, A. Tricyclic Quinoxalines as Potent Kinase Inhibitors of PDGFR Kinase, Flt3 and Kit. *Bioorg. Med. Chem.* **2003**, *11*, 2007−2018; (j) Sun, L.; Liang, C.; Shirazian, S.; Zhou, Y.; Miller, T.; Cui, J.; Fukuda, J. Y.; Chu, J.-Y.; Nematalla, A.; Wang, X.; Chen, H.; Sistla, A.; Luu, T. C.; Tang, F.; Wei, J.; Tang, C. Discovery of 5-[5-Fluoro-2-oxo-1,2-dihydroindol-(3*Z*)-ylidenemethyl]-2,4-dimethyl-1*H*-pyrrole-3-carboxylic Acid (2-Diethylaminoethyl)amide, a Novel Tyrosine Kinase Inhibitor Targeting Vascular Endothelial and Platelet-Derived Growth Factor Receptor Tyrosine Kinase. *J. Med. Chem*. **2003**, *46*, 1116−1119; (k) Matsuno, K.; Nakajima, T.; Ichimura, M.; Giese, N. A.; Yu, J.-C.; Lokker, N. A.; Ushiki, J.; Ide, S.; Oda, S.; Nomoto, Y. Potent and Selective Inhibitors of PDGF Receptor Phosphorylation. 2. Synthesis, Structure Activity Relationship, Improvement of Aqueous Solubility, and Biological Effects of 4-[4-(N-Substituted (thio)carbamoyl)-1-piperazinyl]-6,7-dimethoxyquinazoline Derivatives. *J. Med. Chem*. **2002**, *45*, 4513−4523; (l) Pandey, A.; Volkots, D. L.; Seroogy, J. M.; Rose, J. W.; Yu, J.-C.; Lambing, J. L.; Hutchaleelaha, A.; Hollenbach, S. J.; Abe, K.; Giese, N. A.; Scarborough, R. M. Identification of Orally Active, Potent, and Selective 4-Piperazinylquinazolines as Antagonists of the Platelet-Derived Growth Factor Receptor Tyrosine Kinase Family. *J. Med. Chem.* **2002**, *45*, 3772−3793; (m) Matsuno, K.; Ichimura, M.; Nakajima, T.; Tahara, K.; Fujiwara, S.; Kase, H.; Ushiki, J.; Giese, N. A.; Pandey, A.; Scarborough, R. M.; Lokker, N. A.; Yu, J.-C.; Irie, J.; Tsukuda, E.; Ide, S.-I.; Oda, S.; Nomoto, Y. Potent and Selective Inhibitors of Platelet-Derived Growth Factor Receptor Phosphorylation. 1. Synthesis, Structure−Activity Relationship, and Biological Effects of a New Class of Quinazoline Derivatives. *J. Med. Chem.* **2002**, *45*, 3057−3066; (n) Mahboobi, S.; Teller, S.; Pongratz, H.; Hufsky, H.; Sellmer, A.; Botzki, A.; Uecker, A.; Beckers, T.; Baasner, S.; Schaechtele, C.; Ueberall, F.; Kassack, M. U.; Dove, S.; Boehmer, F.-D. Bis(1H-2-indolyl)methanones as a Novel Class of Inhibitors of the Platelet-Derived Growth Factor Receptor Kinase. *J. Med. Chem.* **2002**, *45*, 1002−1018; (o) Sun, L.; Tran, N.; Liang, C.; Hubbard, S.; Tang, F.; Lipson, K.; Schreck, R.; Zhou, Y.; McMahon, G.; Tang, C. Identification of Substituted 3-[(4,5,6,7-Tetrahydro-1*H*-indol-2-yl)methylene]-1,3-dihydroindol-2-ones as Growth Factor Receptor Inhibitors for VEGF-R2 (Flk-1/KDR), FGF-R1, and PDGF-Rβ Tyrosine Kinases. *J. Med. Chem.* **2000**, *43*, 2655−2663; (p) Palmer, B. D.; Kraker, A. J.; Hartl, B. G.; Panopoulos, A. D.; Panek, R. L.; Batley, B. L.; Lu, G. H.; Trumpp-Kallmeyer, S.; Showalter, H. D. H.; Denny, W. A. Structure−Activity Relationships for 5-Substituted 1-Phenylbenzimidazoles as Selective Inhibitors of the Platelet-Derived Growth Factor Receptor. *J. Med. Chem.* **1999**, *42*, 2373−2382; (q) Palmer, B. D.; Smaill, J. B.; Boyd, M.; Boschelli, D. H.; Doherty, A. M.; Hamby, J. M.; Khatana, S. S.; Kramer, J. B.; Kraker, A. J.; Panek, R. L.; Lu, G. H.; Dahring, T. K.; Winters, R. T.; Showalter, H. D. H.; Denny, W. A. Structure−Activity Relationships for 1-Phenylbenzimidazoles as Selective ATP Site Inhibitors of the Platelet-Derived Growth Factor Receptor. *J. Med. Chem.* **1998**, *41*, 5457−5465; (r) Gazit, A.; App, H.; McMahon, G.; Chen, J.; Levitzki, A.; Bohmer, F. D. Tyrphostins. 5. Potent Inhibitors of Platelet-Derived Growth Factor Receptor Tyrosine Kinase: Structure−Activity Relationships in Quinoxalines, Quinolines, and Indole Tyrphostins. *J. Med. Chem.* **1996**, *39*, 2170−2177; (s) Dolle, R. E.; Dunn, J. A.; Bobko, M.; Singh, B.; Kuster, J. E.; Baizman, E.; Harris, A. L.; Sawutz, D. G.; Miller, D.; Wang, S.; Faltynek, C. R.; Xie, W.; Sarup, J.; Bode, D. C.; Pagani, E. D.; Silver, P. J. 5,7-Dimethoxy-3-(4-pyridinyl)quinoline Is a Potent and Selective Inhibitor of Human Vascular β-Type Platelet-Derived Growth Factor Receptor Tyrosine Kinase. *J. Med. Chem.* **1994**, *37*, 2627−2629.

(29) Jain, R. K. Normalization of Tumor Vasculature: An Emerging Concept in Antiangiogenic Therapy. *Science* **2005**, *307*, 58−62.

(30) Several patents covering indeno[1,2-c]-3-arylpyrazoles have appeared. See: (a) Arnold, L. D.; Xu, Y.; Barlozzari, T. Preparation of indeno[1,2-c]-, naphtho[1,2-c]- and benzo[6,7]cyclohepta[1,2-c]pyrazoles as tyrosine kinase inhibitors. WO 9917769, 1999. (b) Habeck, D. A.; Houlihan, W. J. Substituted indeno, naphtho and cyclohepta pyrazoles. US 3932430, 1976. (c) Coombs, R. V.; Houlihan, W. J. Substituted indeno, naphtho, and cyclohepta pyrazoles. US 3843665, 1974; US 3843666, 1974.

(31) (a) Mei, J.; Tuman, R. W.; Ho, C.; Galemmo, R.; Sechler, J.; Devine, A.; Lu, H.; Garrabrant, T.; Ludovici, D.; Strobel, E.; Maharoof, U.; Tominovich, R.; Voina, S.; Emanuel, S.; Gruninger, R.; Brunmark, A.; Johnson, D. L. A Novel PDGF Receptor Kinase Inhibitor with Dual Anti-Angiogenesis and Tumor Cell Anti-Proliferative Activity. Presented at the Annual Meeting of the American Association of Cancer Research, Orlando, FL, March 27−31, 2004, Abstract #3990. (b) Tuman, R. W.; Mei, J.; Ho, C.; Galemmo, R.; Ludovici, D.; Baker, J.; Burns, C.; Devine, A.; Maharoof, U.; Sechler, J.; Strobel, E.; Tominovich, R.; Skrzat, S.; Voina, S.; Johnson, D. L. Discovery of A Novel, Dual Mechanism Anti-Angiogenic and Anti-Proliferative Agent with Oral Anti-tumor Activity. Presented at the Annual Meeting of the American Association of Cancer Research, Orlando, FL, March 27−31, 2004, Abstract #4558.

(32) (a) Druker, B. J.; Tamura, S.; Buchdunger, E.; Ohno, S.; Segal, G. M.; Fanning, S.; Zimmermann, J.; Lydon, N. B. Effects of a Selective Inhibitor of the Abl Tyrosine Kinase on the Growth of Bcr-Abl Positive Cells *Nature Med.* **1996**, *2*, 561−566; (b) Druker, B. J.; Sawyers, C. L.; Kantarjian, H.; Resta, D. J.; Reese, S. F.; Ford, J. M.; Capdeville, R.; Talpaz, M. Activity of a Specific Inhibitor of the BCR-ABL Tyrosine Kinase in the Blast Crisis of Chronic Myeloid Leukemia and Acute Lymphoblastic Leukemia with the Philadelphia Chromosome *N. Engl. J. Med.* **2001**, *344*, 1038−1042.; (c) Druker, B. J.; Talpaz, M.; Resta, D. J.; Peng, B.; Buchdunger, E.; Ford, J. M.; Lydon, N. B.; Kantarjian, H.; Capdeville, R.; Ohno-Jones, S.; Sawyers, C. L. Efficacy and Safety of a Specific Inhibitor of the BCR-ABL Tyrosine Kinase in Chronic Myeloid Leukemia *N. Engl. J. Med.* **2001**, *344*, 1031−1037; (d) Apperley, J. F.; Gardembas, M.; Melo, J. V.; Russell-

Jones, R.; Bain, B. J.; Baxter, J.; Chase, A.; Chessells, J. M.; Colombat, M.; Dearden, C. E.; Dimitrijevic, S.; Mahon, F.-X.; Marin, D.; Nikolova, Z.; Olavarria, E.; Silberman, S.; Schultheis, B.; Cross, N. C. P.; Goldman, J. M. Response to Imantinib Mesylate in Patients with Chronic Myeloproliferative Diseases with Rearrangements of the Platelet-Derived Growth Factor Receptor-β. *N. Engl. J. Med.* **2002**, *347*, 481−487.

(33) (a) Nugiel, D. A.; Etzkorn, A.-M.; Vidwans, A.; Benfield, P. A.; Boisclair, M.; Burton, C. R.; Cox, S.; Czerniak, P. M.; Doleniak, D.; Seitz, S. Indenopyrazoles as Novel Cyclin Dependent Kinase (CDK) Inhibitors. *J. Med. Chem.* **2001**, *44*, 1334−1336; (b) Nugiel, D. A.; Vidwans, A.; Etzkorn, A.-M.; Rossi, K. A.; Benfield, P. A.; Burton, C. R.; Cox, S.; Doleniak, D.; Seitz, S. Synthesis and Evaluation of Indenopyrazoles as Cyclin-Dependent Kinase Inhibitors. 2. Probing the Indeno Ring Substitution Pattern. *J. Med. Chem.* **2002**, *45*, 5224−5232; (c) Yue, E. W.; Higley, A. C.; DiMeo, S. V.; Carini, D. J.; Nugiel, D. A.; Benware, C.; Benfield, P. A.; Burton, C. R.; Cox, S.; Grafstrom, R. H.; Sharp, D. M.; Sisk, L. M.; Boylan, J. F.; Muckelbauer, J. K.; Smallwood, A. M.; Chen, H.; Chang, C.-H.; Seitz, S. P.; Trainor, G. L. Synthesis and Evaluation of Indenopyrazoles as Cyclin-Dependent Kinase Inhibitors. 3. Structure Activity Relationships at C3. *J. Med. Chem.* **2002**, *45*, 5233−5248.

(34) McTigue, M. A.; Wickersham, J. A.; Pinko, C.; Showalter, R. E.; Parast, C. V.; Tempczyk-Russell, A.; Gehring, M. R.; Mroczkowski, B.; Kan, C.-C.; Villafranca, J. E.; Appelt, K. Crystal Structure of the Kinase Domain of Human Vascular Endothelial Growth Factor Receptor 2: A Key Enzyme in Angiogenesis. *Structure* **1999**, *7*, 319−330.

(35) For **17** dissolved in DMSO-d_6 the 1D proton spectrum showed two resonances for each of the NH protons in a 3:1 ratio, and this doubling was also observed for the fluorophenyl aromatic protons and the methylene protons on the dihydroindeno[1,2-*c*]-pyrazole ring system. The singlets for the methoxy protons attached at C-6 and the methylene protons on C-4 were broadened. The ROESY spectrum showed exchange peaks between the two sets of resonances. There was an ROE from the downfield NH to H8 confirming its assignment as the pyrazole NH at the 1-position. This was confirmed by a 2D [^{1}H]−[^{15}N] gradient-HMBC experiment that gave a 3-bond correlation from the major aniline NH to the major pyrazole N2. The HMBC experiment did not suppress the one bond NH coupling so doublets were observed for the N1 and aniline nitrogens. Proton−nitrogen correlations were not observed for the minor isomer. In the 2D [^{1}H]−[^{13}C] gradient-HMBC data the pyrazole NH did not show correlations to carbons outside of the pyrazole ring and thus could not be used to further confirm the ROESY results. ROEs were seen from the aniline NH and the fluoroaromatic protons to the methylene protons on the dihydroindeno-[1,2-*c*]pyrazole ring, suggesting that both the "in" and "out" orientations were accessible on the NMR time scale. Hindered rotation about the aniline−NH−pyrazole bond is believed to be the cause for the doubling of the resonances. The proton spectra of **17** in $CDCl_3$ or AcCN-d_3 did not show a doubling of the resonances as observed in DMSO-d_6. In deuteriochloroform the NH resonances were broadened almost into the baseline and in deuterioacetonitrile the NH resonances were broad, as well, as one of the fluorophenyl protons. For a full disclosure of the experimental details, see the Supporting Information.

(36) Stamos, J.; Sliwkowski, M. X.; Eigenbrot, C. Structure of the Epidermal Growth Factor Receptor Kinase Domain Alone and in Complex with a 4-Anilinoquinazoline Inhibitor. *J. Biol. Chem.* **2002**, *277*, 46265−72.

(37) Gorre, M. E.; Mohammed, M.; Ellwoood, K.; Hsu, N.; Paquette, R.; Rao, P. N.; Sawyers, C. L. Clinical Resistance to STI-571 Cancer Chemotherapy Caused by BCR-ABL Gene Mutation or Amplification *Science* **2001**, *293*, 876−880.

(38) Emanuel, S.; Gruninger, R. H.; Fuentes-Pesquera, A.; Connolly, P. J.; Seamon, J. A.; Hazel, S.; Tominovich, R.; Hollister, B.; Napier, C.; D'Andrea, M. R.; Reuman, M.; Bignan, G.; Tuman, R.; Johnson, D.; Moffatt, D.; Batchelor, M.; Foley, A.; O'Connell, J.; Allen, R.; Perry, M.; Jolliffe, L.; Middleton, S. A. A Vascular Endothelial Growth Factor Receptor-2 Kinase Inhibitor Potentiates the Activity of the Conventional Chemotherapeutic Agents Paclitaxel and Doxorubicin in Tumor Xenograft Models, *Mol. Pharmacology* **2004**, *66*, 635−647.

JM050680M